Outage Performance of NOMA-based DF Relay Sharing Networks over *Nakagami-m* Fading Channels

Shady M. Ibraheem [1,2], Walid Bedawy [1]

[1] Electronics and Electrical Comm. Dep., Faculty of Electronic Engineering, Menoufia University, Egypt.
[2] Telecom Egypt, Egypt.
(e-mail: shadymam;walidbedawy@gmail.com).

Waleed Saad [1,3] and Mona Shokair [1]

[3] Electrical Engineering Department, College of Engineering, Shaqra University, Dawadmi, Ariyadh, KSA.
(e-mail: waleed.saad @el-eng.menofia.edu.eg; mona.sabry @el-eng.menofia.edu.eg).

***Abstract*—In this paper, we study the performance of cooperative non-orthogonal multiple access (C-NOMA) spectrum-sharing networks with a decode-and-forward (DF) relay over *Nakagami-m* Fading Channels. Two sources are paired to perform NOMA and transmit information to two paired destinations in the opposite direction via one shared half-duplex (HD) DF relay. New closed-form expressions for the outage probability, the asymptotic outage probability and the system throughput, as performance metrics, are derived over such a channel fading model. Simulation results investigate the correctness of our derivations and demonstrate the impact of the fading parameters and average channel coefficients on the performance.**

Keywords*—Cooperative non-orthogonal multiple access (C-NOMA); outage probability; spectrum sharing and decode-and-forward (DF) relay.

I. INTRODUCTION

Non-orthogonal multiple access (NOMA) is recently receiving a considerable attention as a promising technique to achieve higher spectral efficiency of the fifth generation (5G) mobile communication networks [1]-[2]. The downlink multi-user superposition transmission (MUST) NOMA technique has also been included in the Third Generation Partnership Project (3GPP) Long Term Evolution-Advanced (LTE-A) standard ([3] and references therein). The key idea of NOMA is to enable multiple users to transmit/receive at the same time/frequency/code resource but with different power levels. The receivers of better channel conditions perform successive interference cancellation (SIC) mechanism to separate superimposed signals of the poorer ones before decoding their own signals. Compared to OMA, NOMA can offer a significant improvement in both spectrum efficiency and user fairness with flexible user scheduling and bandwidth assignment [4]. To reduce the complexity of the encoding/decoding processes user pairing was proposed in [5] where the users can be classified into orthogonal groups of two users to reduce the complexity.

Cooperative NOMA is an effective approach to enhance the transmission reliability for the user of poor channel condition by exploiting the spatial diversity [6]. In cooperative NOMA, the near users act as a relay to improve the reliability of the far users ([7] and references therein) while in the applications of NOMA into cooperative networks a dedicated relay is employed [8]-[10]. In context of the applications of NOMA utilizing DF relay, the authors in [8] derived the achievable capacity of a DF relay assisted NOMA multiplexed system as performance metrics. While in [9]-[10] the applications of NOMA into cooperative *half-duplex* (HD) and *full-duplex* (FD) relay was investigated in where analytical expressions for the outage probability and ergodic sum rate were derived.

Comparing with Rayleigh fading considered in the above literature, *Nakagami-m* fading model provides better matching to numerous empirical data measurements [11]. Therefore, a downlink NOMA based amplify-and- forward (AF) relaying system over *Nakagami-m* fading channels was investigated in [12] where the authors derived an explicit expression for the outage probability and the lower and upper bounds of the ergodic sum rate while the outage of a fixed gain NOMA based AF relay system was analysed in [13]. However, in [9]-[10] the application of NOMA into spectrum sharing network under a generalized fading model has not been reported and justified which motivates our work.

In this paper, we study a user paired uplink-downlink cooperative NOMA sharing system through a shared DF relay over *Nakagami-m* fading channels. New closed-form and asymptotic expressions for the outage probability of the system are derived where the impact of the fading parameters and channel coefficients are studied. We show that the outage behavior of our system is superior to that of orthogonal multiple access (OMA)-based system in terms of outage throughput in delay limited transmission systems.

II. SYSTEM AND CHANNEL MODELS

In this section, we consider two phases NOMA-based cooperative relay network where two sources, i.e., A_1 and A_2,

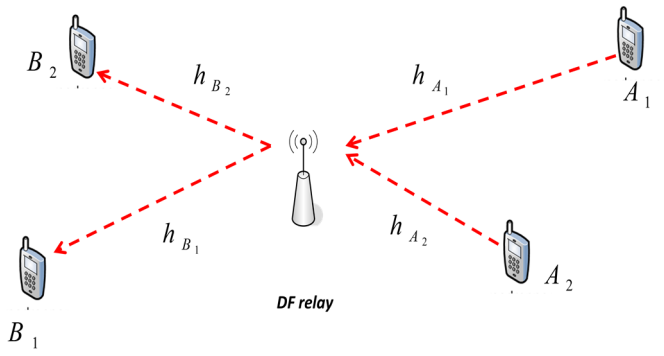

Fig. 1. The system model.

are paired to perform NOMA[1] to simultaneously transmit their own information to a corresponding pair of destinations, i.e., B_1 and B_2 through a shared HD relay employing DF relaying protocol, as shown in Fig. 1. The direct links from A_1 and A_2 to B_1 and B_2 are assumed to be unavailable due to multipath shadowing effects as justified in [12]. All nodes are equipped with a single antenna and operate in HD mode. For mathematical tractability, two disjunct pair of users are considered where each pair is clustered such that cell-edge users, A_1 and B_1, are paired with cell-center users, A_2 and B_2, respectively, as in conventional random NOMA user pairing [5]. We consider (as in [7]) perfect CSIs acquired by all receiving nodes where all the channels are assumed to be modeled as independent and non-identical *Nakagami-m* fading distributions[2] which mean that $\gamma_i = |h_i|^2 \sim \mathcal{G}(m_i, \lambda_i)$ follows gamma distributions with fading parameters m_i and average channel powers λ_i, i.e., $\lambda_i = \mathbb{E}\{|h_i|^2\}$, where h_i is the channel fading coefficient between the node $i, i \in \{A_1, A_2, B_1, B_2\}$ and the HD-DF relay. Without loss of generality, the fading coefficients are arranged [10] as $h_{A_1} < h_{A_2}$ and $h_{B_1} < h_{B_2}$. Information transmission comprises two phases (two time slots) described as follows.

A. First Phase

In this phase, both A_1 and A_2 transmit simultaneously the symbols x_1 and x_2 with distributed power allocation coefficients a_1 and a_2, respectively, where $a_1 + a_2 = 1$. The DF relay receives the superimposed symbols at the same time by employing a specific type of synchronized time detection network coding (NC). Both a_1 and a_2 are determined such that the received signal to noise ratio (SNR) at the DF relay satisfy $|h_{A_1}|^2 \rho a_1 < |h_{A_2}|^2 \rho a_2$, or $a_1 < |h_{A_2}|^2/(|h_{A_1}|^2 + |h_{A_2}|^2)$, where ρ is the transmit SNR, i.e., $\rho \triangleq \frac{P}{N_0}$, N_0 is the thermal noise variance of the receiving nodes.

[1]It is considered that A_1 and A_2 undergo a power distribution system and contribute a total sum of transmit powers, i.e., P.

[2]The channel coefficients keep constants within one time slot but change independently over the successive time slots.

Therefore, as in uplink NOMA, the relay tries to decode the symbol x_2 of a strong channel condition by treating the symbol x_1 of a weak channel condition as a noise. Then, it cancels x_2 from the superimposed signals using successive interference cancellation (SIC) to acquire x_1. Consequently, the SNR arrived at the relay to detect the symbol x_2 can be given by

$$\gamma_{x_2}^{(1)} = \frac{a_2 \rho |h_{A_2}|^2}{a_1 \rho |h_{A_1}|^2 + 1}, \quad (1)$$

where x_1 and x_2 are assumed to be normalized unity power symbols, i.e., $\mathbb{E}\{x_1^2\} = \mathbb{E}\{x_2^2\} = 1$.

After applying SIC ([6] and [8]), the SNR recovered for the symbols x_1 can be obtained as

$$\gamma_{x_1}^{(1)} = a_1 \rho |h_{A_1}|^2. \quad (2)$$

B. Second Phase

In this phase, after decoding x_1 and x_2, the DF relay re-encodes them one more time by retransmitting a superimposed signal $y = x_1\sqrt{P_r b_1} + x_2\sqrt{P_r b_2}$, with different power allocation coefficients b_1 and b_2 to ensure fairness between the received nodes B_1 and B_2, respectively, where $b_1 + b_2 = 1$, $b_1 > b_2$ and $P_r \triangleq P$ is the transmit power of the relay.

Following the NOMA principle, B_1 decodes the symbol x_1 by treating x_2 as a noise. Therefore, the received SNR at B_1 can be expressed as

$$\gamma_{x_1}^{(2)} = \frac{b_1 \rho |h_{B_1}|^2}{b_2 \rho |h_{B_1}|^2 + 1}. \quad (3)$$

B_2 can successfully detect x_1 by treating its own symbol x_2 as interference. Then, it perform SIC to subtract x_1 from the received signal before extracting x_2. Thus, the received SNR at B_2 to extract both x_1 and x_2 can be, respectively, given by

$$\gamma_{x_1 \to x_2}^{(2)} = \frac{b_1 \rho |h_{B_2}|^2}{b_2 \rho |h_{B_2}|^2 + 1}, \quad (4)$$

$$\gamma_{x_2}^{(2)} = b_2 \rho |h_{B_2}|^2. \quad (5)$$

III. OUTAGE PERFORMANCE ANALYSIS

The outage probability is considered as a significant performance metric when the target rates at the destinations are determined by certain quality of service (QoS) requirements. The probability density function (PDF) of $\gamma_i, i \in \{A_1, A_2, B_1, B_2\}$, can be expressed as [11]

$$f_{\gamma_i}(\gamma) = \left(\frac{m_i}{\lambda_i}\right)^{m_i} \frac{\gamma^{m_i - 1}}{\Gamma(m_i)} e^{-\frac{m_i \gamma}{\lambda_i}}, \quad (6)$$

where m_i is an integer greater than one. By utilizing the series expansion of incomplete Gamma function the cumulative density function (CDF) of γ_i is given by

$$F_{\gamma_i}(\gamma) = 1 - e^{-\frac{m_i \gamma}{\lambda_i}} \sum_{k=0}^{m_i - 1} \frac{1}{k!} \left(\frac{m_i \gamma}{\lambda_i}\right)^k \quad (7)$$

.

Let $\gamma_{th}^{(1)}$ and $\gamma_{th}^{(2)}$ be the minimum acceptable SNRs to transmit x_1 and x_2, respectively, where $\gamma_{th}^{(l)} \triangleq 2^{2R_{th}^{(l)}} - 1$, $l \in \{1,2\}$ and $R_{th}^{(l)}$ represents a predetermined target rate.

A. Exact Outage Probability of $A_1 \to B_1$ Communication

The outage event occurs when B_1 is not able to decode x_1 which can be formulated as

$$P_{out}^{A_1 \to B_1} = 1 - Pr\left(\gamma_{x_2}^{(1)} > \gamma_{th}^{(2)}, \gamma_{x_1}^{(1)} > \gamma_{th}^{(1)}, \gamma_{x_1}^{(2)} > \gamma_{th}^{(1)}\right) \quad (8)$$

The following theorem gives the outage probability at B_1.

Theorem 1*: A closed-form expression for $P_{out}^{A_1 \to B_1}$ is given by (9) at the top of the next page, where $\tau_1 = \frac{m_{A_1}}{\lambda_{A_1} a_1}$, $\tau_2 = \frac{m_{A_2}}{\lambda_{A_2} a_2}$, $\tau_3 = \frac{m_{B_1}}{\lambda_{B_1}} \frac{\gamma_{th}^{(1)}}{\left(b_1 - b_2 \gamma_{th}^{(1)}\right)}$ with $\gamma_{th}^{(1)} < \frac{b_1}{b_2}$ and $\binom{n}{r} = \frac{n!}{(n-r)!r!}$.*

Proof: See Appendix A.

B. Exact Outage Probability of $A_2 \to B_2$ Communication

In this case, the outage event occurs when B_2 is not able to decode x_2 which can be given as

$$P_{out}^{A_2 \to B_2} = 1 - \Pr(\gamma_{x_2}^{(1)} > \gamma_{th}^{(2)}, \gamma_{x_1 \to x_2}^{(2)} > \gamma_{th}^{(1)}, \gamma_{x_2}^{(2)} > \gamma_{th}^{(2)}). \quad (10)$$

The following theorem gives the outage probability at B_2.

Theorem 2*: A closed-form expression for $P_{out}^{A_2 \to B_2}$ is given by (11) at the top of the next page, where $\tau^* = \frac{m_{B_2}}{\lambda_{B_2}} \delta^*$, $\gamma_{th}^{(1)} < \frac{a_2}{a_1}$ and $\delta^* \triangleq max\left(\gamma_{th}^{(1)} / \left(b_1 - b_2 \gamma_{th}^{(1)}\right), \gamma_{th}^{(2)} / b_2\right)$.*

Proof: See Appendix B.

To give more insights on the performance of the system, we investigate the impact of increasing ρ on the outage probability of the two communication pairs as follows.

C. Asymptotic Outage Probability of $A_1 \to B_1$ Communication

As $\rho \to \infty$, $e^{-x} \approx 1 - x$, the CDF of γ_i can be approximated to

$$F_{\gamma_i}^{\infty}(\gamma) = \frac{(m_i \gamma / \lambda_i)^{m_i}}{m_i!}. \quad (12)$$

Based on (8), an asymptotic outage probability expression can be given by $P_{out_\infty}^{A_1 \to B_1} = 1 - \Theta_1^{\infty} \Theta_2^{\infty}$, where Θ_2^{∞} is expressed as an approximate as

$$\Theta_2^{\infty} = \frac{(\tau_3 / \rho)^{m_{B_1}}}{m_{B_1}!}, \quad (13)$$

while Θ_1^{∞} can be determined by plugging $F_{\gamma_{A_1}}^{\infty}(\gamma)$ of m_{A_1} into (**A.3**). Then, by solving the integral, from (10) and performing some algebraic manipulations, $\Theta_1^{\infty} = \Theta_3^{\infty} - F_{\gamma_{A_1}}\left(\frac{\gamma_{th}^{(1)}}{a_1 \rho}\right)\left(1 - F_{\gamma_{A_2}}\left(\frac{\gamma_{th}^{(2)}}{a_2 \rho}\right)\right)$, where $\Theta_3^{\infty} \triangleq \int_{\gamma_{th}^{(2)}/a_2\rho}^{\infty} \left(\frac{m_{A_2}}{\lambda_{A_2}}\right)^{m_{A_2}} \frac{x^{m_{A_2}-1}}{m_{A_1}! m_{A_2}-1!} \times e^{-\frac{m_{A_2} x}{\lambda_{A_2}}} \left(\frac{m_{A_1}}{\lambda_{A_1}} \frac{a_2 x - \gamma_{th}^{(2)}/\rho}{a_1 \gamma_{th}^{(2)}}\right)^{m_{A_1}} dx$, $\Theta_3^{\infty} =$

$$\frac{\left(\frac{\tau_2}{\tau_1}\gamma_{th}^{(2)}\right)^{m_{A_2}-m_{A_1}}}{m_{A_1}!\left(m_{A_2}-1\right)!}\left(\frac{m_{A_1}}{\lambda_{A_1}}\right)^{m_{A_1}}\left(1 - \tau_2 \frac{\gamma_{th}^{(2)}}{\rho}\right) \times \sum_{l=0}^{m_{A_2}-1} \binom{m_{A_2}-1}{l} \left(\frac{\tau_1}{\rho}\right)^{m_{A_2}-l-1} \frac{\left(m_{A_1}+l\right)!}{\left(\frac{\tau_2}{\tau_1}\gamma_{th}^{(2)}\right)^{l+1}} \quad (14)$$

Remark 1. To obtain further insights, we consider the achievable diversity order which is defined as $d = -\lim_{\rho \to \infty}\left(P_{out_\infty}^{A_1 \to B_1} / \log \rho\right)$ to investigate the benefits of cooperative NOMA. It is clear from (13-14) that $P_{out_\infty}^{A_1 \to B_1} \propto \rho^{-min\left(m_{A_1}, m_{A_2}, m_{B_1}\right)}$, which means that a diversity order of $min\left(m_{A_1}, m_{A_2}, m_{B_1}\right)$ can be achieved at B_1. It is noted that the diversity order may be dominated by m_{A_2} imposed by the detection of x_2 firstly in the uplink NOMA transmission.

D. Asymptotic Outage Probability of $A_2 \to B_2$ Communication

Following (9) and applying similar steps as in *Subsection* ***C***, an asymptotic outage probability expression can be expressed as $P_{out_\infty}^{A_2 \to B_2} = 1 - \Theta_4^{\infty} \Theta_5^{\infty}$, where Θ_5^{∞} is given from (**B.2**) as

$$\Theta_5^{\infty} = \frac{(\tau^* / \rho)^{m_{B_2}}}{m_{B_2}!}, \quad (15)$$

while Θ_4^{∞} is derived as (12), i.e., $\Theta_4^{\infty} \triangleq \Theta_3^{\infty}$.

Remark 2. It is clear that $P_{out_\infty}^{A_2 \to B_2} \propto \rho^{-min\left(m_{A_2}, m_{B_2}\right)}$, which means that a diversity order of $min\left(m_{A_2}, m_{B_2}\right)$ can be achieved at B_2.

E. System Throughput Analysis

In the delay-limited communication systems, if the transmit nodes sends information at fixed rate, the system throughput can be evaluated by the outage probability. Thus, the overall system throughput rate can be expressed as

$$\mathcal{R} = \left(1 - P_{out}^{A_1 \to B_1}\right) R_{th}^{(1)} + \left(1 - P_{out}^{A_2 \to B_2}\right) R_{th}^{(2)}. \quad (16)$$

IV. SIMULATION RESULTS

In this section, a comparison is performed between the user paired cooperative NOMA spectrum-sharing system for both *Nakagami-m* and *Rayleigh* fading channels [9] and the conventional OMA based system where the better communication pair is scheduled.

Without loss of generality, the main parameters are set as $R_{th}^{(1)} = R_{th}^{(2)} = 0.5\ bps/Hz$, $\lambda_{A_1} = 0.5$, $\lambda_{A_2} = 1$, $\lambda_{B_1} = 0.5$,

$$P_{out}^{A_1\to B_1} = 1 - exp\left(-\left(\frac{\gamma_{th}^{(1)}}{\rho}\tau_1 + \frac{\gamma_{th}^{(2)}}{\rho}\tau_2 + \frac{\tau_3}{\rho}\right)\right)\sum_{k=0}^{m_{A_1}-1}\frac{1}{k!}\left(\frac{\gamma_{th}^{(1)}}{\rho}\tau_1\right)^k\sum_{l=0}^{m_{A_2}-1}\frac{1}{l!}\left(\frac{\gamma_{th}^{(2)}}{\rho}\tau_2\right)^l$$
$$\times\sum_{k=0}^{m_{B_1}-1}\frac{1}{k!}\left(\frac{\tau_3}{\rho}\right)^k - \frac{\left(\frac{\tau_2}{\tau_1}\gamma_{th}^{(2)}\right)^{m_{A_2}}}{(m_{A_2}-1)!}exp\left(-\left(\frac{\gamma_{th}^{(2)}}{\rho}\tau_2 + \frac{\tau_3}{\rho}\right)\right)\sum_{k=0}^{m_{B_1}-1}\frac{1}{k!}\left(\frac{\tau_3}{\rho}\right)^k\sum_{l=0}^{m_{A_2}-1}\binom{m_{A_2}-1}{l}$$
$$\times\left(\frac{\tau_1}{\rho}\right)^{m_{A_2}-l-1}\sum_{k=0}^{m_{A_1}-1}\frac{1}{k!}\frac{(k+l)!}{\left(\frac{\tau_2}{\tau_1}\gamma_{th}^{(2)}+1\right)^{l+k+1}} \quad \textbf{(9)}$$

$$P_{out}^{A_2\to B_2} = 1 - \frac{\left(\frac{\tau_2}{\tau_1}\gamma_{th}^{(2)}\right)^{m_{A_2}}}{(m_{A_2}-1)!}exp\left(-\left(\frac{\gamma_{th}^{(2)}}{\rho}\tau_2 + \frac{\tau^*}{\rho}\right)\right)\times$$
$$\sum_{k=0}^{m_{B_1}-1}\frac{1}{k!}\left(\frac{\tau^*}{\rho}\right)^k\sum_{l=0}^{m_{A_2}-1}\binom{m_{A_2}-1}{l}\left(\frac{\tau_1}{\rho}\right)^{m_{A_2}-l-1}\sum_{k=0}^{m_{A_1}-1}\frac{1}{k!}\frac{(k+l)!}{\left(\frac{\tau_2}{\tau_1}\gamma_{th}^{(2)}+1\right)^{l+k+1}} \quad \textbf{(11)}$$

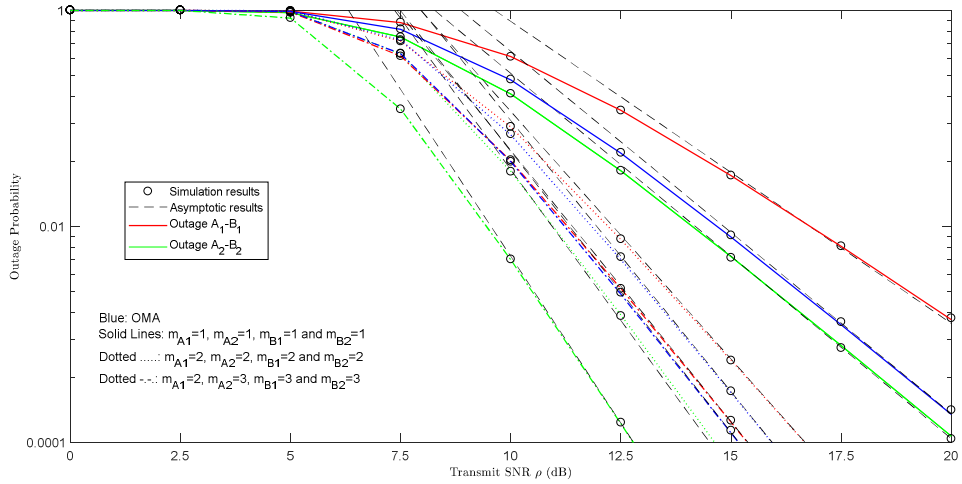

Fig. 2. Outage probability versus transmit SNR ρ for selected values of m_i.

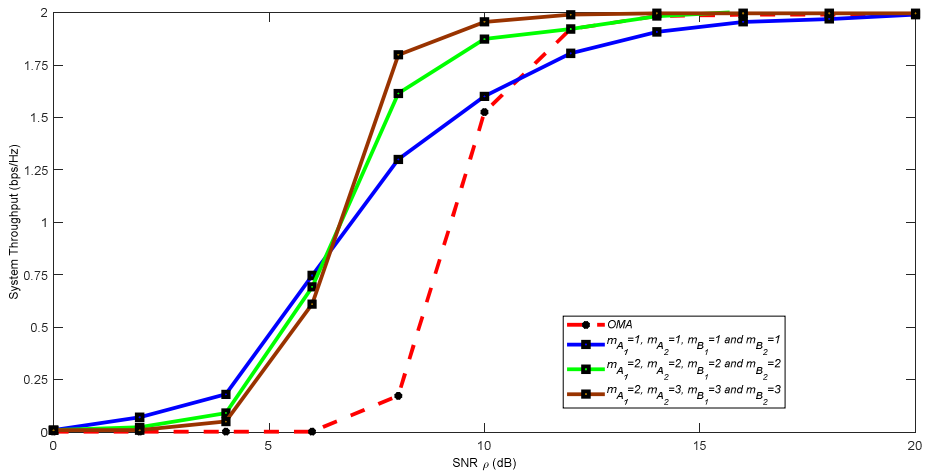

Fig. 3. System throughput in delay-limited mode versus ρ.

$\lambda_{B_2} = 1$, $a_1 = 0.4$, $a_2 = 0.6$, $b_1 = 0.7$ and $b_2 = 0.3$, while in the conventional OMA based system as a benchmark, the target rate can be considered as $R_{th}^{(0)} = R_{th}^{(1)} + R_{th}^{(2)}$ where we assume an equal power allocation coefficient to each source.

In Fig. 2, the cooperative NOMA spectrum-sharing scheme can achieve lower outage performance over the conventional OMA based scheme as a function of the transmit SNR, i.e., ρ, with the increasing values of $m_i, i \in \{A_1, A_2, B_1, B_2\}$. As can be observed, the *Nakagami-m* fading model adds degrees of freedom on the possibility of detecting both x_1 and x_2 over the Rayleigh fading model [9], i.e., $m_i = 1$. It is worth pointing that the high SNR slope for outage probability, i.e., diversity order, is becoming larger where large m_i results in a higher diversity order. Furthermore, the performance is dominated significantly by the smallest value of m_i. Obviously, the analytical results are in a good agreement with Monte Carlo simulation results.

Fig. 3 depicts the system throughput versus SNR in the delay-limited communication mode. It is obvious that the *Nakagami-m* fading model can achieve the higher system throughput due to its lower outage probability. At high SNR, the slope of throughputs converges to a ceiling value since the outage approaches zero. Thus, the system throughput is only determined by target rates.

V. CONCLUSIONS

This paper studies a user paired uplink-downlink cooperative NOMA sharing system over *Nakagami-m* fading channels. New formulas for the outage probability and the system throughput of the communicated pair have been derived. It has been investigated how far the fading parameters have a substantial impact on the performance of the system over both NOMA and OMA Rayleigh fading models.

REFERENCES

[1] NTT Docomo. (2014). 5G Radio Access: Requirements, Concept and Technologies. NTT DOCOMO White Paper (pp. 1–13). https://www.nttdocomo.co.jp/english/binary/pdf/corporate/technology/whitepaper_5g/DOCOMO_5G_White_Paper.pdf

[2] Saito, Yuya & Kishiyama, Yoshihisa & Benjebbour, Anass & Nakamura, Takehiro & Li, Anxin & Higuchi, Kenichi. (2013). Non-Orthogonal Multiple Access (NOMA) for Cellular Future Radio Access. 1-5, https://doi.org/10.1109/VTCSpring.2013.6692652

[3] Z. Ding, X. Lei, G. K. Karagiannidis, R. Schober, J. Yuan and V. K. Bhargava, "A Survey on Non-Orthogonal Multiple Access for 5G Networks: Research Challenges and Future Trends," in *IEEE Journal on Selected Areas in Communications*, vol. 35, no. 10, pp. 2181-2195, Oct. 2017, https://doi.org/10.1109/JSAC.2017.2725519

[4] S. Timotheou and I. Krikidis, "Fairness for Non-Orthogonal Multiple Access in 5G Systems," in *IEEE Signal Processing Letters*, vol. 22, no. 10, pp. 1647-1651, Oct. 2015, https://doi.org/10.1109/LSP.2015.2417119

[5] Z. Ding, P. Fan and H. V. Poor, "Impact of User Pairing on 5G Nonorthogonal Multiple-Access Downlink Transmissions," in *IEEE Transactions on Vehicular Technology*, vol. 65, no. 8, pp. 6010-6023, Aug. 2016, https://doi.org/10.1109/TVT.2015.2480766

[6] Z. Ding, M. Peng and H. V. Poor, "Cooperative Non-Orthogonal Multiple Access in 5G Systems," in *IEEE Communications Letters*, vol. 19, no. 8, pp. 1462-1465, Aug. 2015, https://doi.org/10.1109/LCOMM.2015.2441064

[7] Zhang, Zhengquan & Ma, Zheng & Xiao, Ming & Ding, Zhiguo & Fan, Pingzhi. (2016). Full-Duplex Device-to-Device Aided Cooperative Non-Orthogonal Multiple Access. IEEE Transactions on Vehicular Technology. 66. 1-1, https://doi.org/10.1109/TVT.2016.2600102

[8] J. B. Kim and I. H. Lee, "Capacity analysis of cooperative relaying systems using non-orthogonal multiple access," *IEEE Commun. Lett.*, vol. 19, no. 11, pp. 1949–1952, Nov. 2015, https://doi.org/10.1109/LCOMM.2015.2472414

[9] M. F. Kader, M. B. Shahab, and S. Y. Shin, "Exploiting non-orthogonal multiple access in cooperative relay sharing," *IEEE Commun. Lett.*, vol. 21, no. 5, pp. 1159–1162, May 2017, https://doi.org/10.1109/LCOMM.2017.2653777

[10] M. F. Kader, S. Y. Shin and V. C. M. Leung, "Full-Duplex Non-Orthogonal Multiple Access in Cooperative Relay Sharing for 5G Systems," in *IEEE Transactions on Vehicular Technology*, vol. 67, no. 7, pp. 5831-5840, July 2018, https://doi.org/10.1109/TVT.2018.2799939

[11] Z. Kang, K. Yao, and F. Lorenzelli, "Nakagami-m fading modeling in the frequency domain for OFDM system analysis," *IEEE Commun. Lett.*, vol. 7, no. 10, pp. 484-486, Oct. 2003, https://doi.org/10.1109/LCOMM.2003.818881

[12] J. Men, J. Ge, and C. Zhang, "Performance analysis of non-orthogonal multiple access for relaying networks over nakagami-*m* fading channels," *IEEE Trans. Veh. Technol.*, vol. 66, no. 2, pp. 1200–1208, Feb. 2017, https://doi.org/10.1109/TVT.2016.2555399

[13] X. Yue, Y. Liu, S. Kang, and A. Nallanathan, "Performance analysis of NOMA with fixed gain relaying over Nakagami-*m* fading channels," *IEEE Access*, vol. 5, pp. 5445–5454, Mar. 2017, https://doi.org/10.1109/ACCESS.2017.2677504

[14] Gradshteyn, I. S., & Ryzhik, I. M. (2007). A. Jeffrey, D. Zwillinger (Eds.), Table of integrals, series, and products (7th ed.); Publication Date: March 9, 2007, ISBN-10: 0123736374, ISBN-13: 978-0123736376, ISBN-13: 978-0123736376.

APPENDIX A

Recall $\gamma_i \triangleq |h_i|^2 \sim \mathcal{G}(m_i, \lambda_i)$ and according to (1-3), $P_{out}^{A_1 \to B_1}$ can be rewritten as

$$P_{out}^{A_1\to B_1} = 1 - \Pr\left(\frac{a_2\rho|h_{A_2}|^2}{a_1\rho|h_{A_1}|^2+1} > \gamma_{th}^{(2)}, a_1\rho|h_{A_1}|^2 > \gamma_{th}^{(1)}\right) \times Pr\left(\frac{b_1\rho|h_{B_1}|^2}{b_2\rho|h_{B_1}|^2+1} > \gamma_{th}^{(1)}\right) =$$

$$\underbrace{1 - Pr\left(\frac{a_2|h_{A_2}|^2 - \frac{\gamma_{th}^{(2)}}{\rho}}{a_1\gamma_{th}^{(2)}} > |h_{A_1}|^2 > \frac{\gamma_{th}^{(1)}}{a_1\rho}\right)}_{\Theta_1} \times \underbrace{Pr\left(|h_{B_1}|^2 > \frac{\gamma_{th}^{(1)}}{\rho\left(b_1 - b_2\gamma_{th}^{(1)}\right)}\right)}_{\Theta_2} \quad \textbf{(A.1)}$$

where $b_2\gamma_{th}^{(1)} < b_1$ or $a_2 > \frac{\gamma_{th}^{(2)}}{|h_{A_2}|^2\rho}$, otherwise, $\Theta_2 \triangleq 1$ or $\Theta_1 \triangleq 1$. Thus, Θ_2 and Θ_1 are as

$$\Theta_2 = 1 - F_{\gamma_{B_1}}\left(\frac{\tau_3}{\rho}\right) = exp\left(-\frac{\tau_3}{\rho}\right)\sum_{k=0}^{m_{B_1}-1}\frac{1}{k!}\left(\frac{\tau_3}{\rho}\right)^k \quad \textbf{(A.2)}$$

$$\Theta_1 = \int_{\gamma_{th}^{(2)}/a_2\rho}^{\infty}\int_{\gamma_{th}^{(1)}/a_1\rho}^{\left(a_2x-\gamma_{th}^{(2)}/\rho\right)/a_1\gamma_{th}^{(2)}} f_{\gamma_{A_1}}(y)f_{\gamma_{A_2}}(x)dydx = \int_{\gamma_{th}^{(2)}/a_2\rho}^{\infty} f_{\gamma_{A_2}}(x)\left(F_{\gamma_{A_1}}\left(\frac{a_2x-\gamma_{th}^{(2)}/\rho}{a_1\gamma_{th}^{(2)}}\right) - F_{\gamma_{A_1}}\left(\frac{\gamma_{th}^{(1)}}{a_1\rho}\right)\right)dx \quad \textbf{(A.3)}$$

$$= exp\left(-\left(\frac{\gamma_{th}^{(1)}}{\rho}\tau_1 + \frac{\gamma_{th}^{(2)}}{\rho}\tau_2\right)\right)\sum_{k=0}^{m_{A_1}-1}\frac{1}{k!}\left(\frac{\gamma_{th}^{(1)}}{\rho}\tau_1\right)^k \times \sum_{l=0}^{m_{A_2}-1}\frac{1}{l!}\left(\frac{\gamma_{th}^{(2)}}{\rho}\tau_2\right)^l - \Theta_3$$

, respectively, where $\Theta_3 = \left(\frac{m_{A_2}}{\lambda_{A_2}}\right)^{m_{A_2}} \times$

$$\int_{\gamma_{th}^{(2)}/a_2\rho}^{\infty}\frac{x^{m_{A_2}-1}}{\Gamma(m_{A_2})}e^{-\frac{m_{A_2}x}{\lambda_{A_2}}}exp\left(-\frac{m_{A_1}}{\lambda_{A_1}}\frac{a_2x-\gamma_{th}^{(2)}/\rho}{a_1\gamma_{th}^{(2)}}\right) \times \sum_{k=0}^{m_{A_1}-1}\frac{1}{k!}\left(\frac{m_{A_1}}{\lambda_{A_1}}\frac{a_2x-\gamma_{th}^{(2)}/\rho}{a_1\gamma_{th}^{(2)}}\right)^k dx$$

After substituting $y = \frac{m_{A_1}}{\lambda_{A_1}}\frac{a_2x-\gamma_{th}^{(2)}/\rho}{a_1\gamma_{th}^{(2)}}$ with the aid of [14, 3.351.3], Θ_3 can be given as $\Theta_3 =$

$$\frac{\left(\frac{\tau_2}{\tau_1}\gamma_{th}^{(2)}\right)^{m_{A_2}}}{(m_{A_2}-1)!}exp\left(-\tau_2\frac{\gamma_{th}^{(2)}}{\rho}\right) \times \sum_{l=0}^{m_{A_2}-1}\binom{m_{A_2}-1}{l}\left(\frac{\tau_1}{\rho}\right)^{m_{A_2}-l-1}\sum_{k=0}^{m_{A_1}-1}\frac{1}{k!}\frac{(k+l)!}{\left(\frac{\tau_2}{\tau_1}\gamma_{th}^{(2)}+1\right)^{l+k+1}} \quad \textbf{(A.4)}$$

Substituting (**A.4**), (**A.3**) and (**A.2**) into (**A.1**), (9) can be obtained. The proof is completed.

APPENDIX B

Recall $\gamma_i \triangleq |h_i|^2 \sim \mathcal{G}(m_i, \lambda_i)$ and according to (1) and (4-5), $P_{out}^{A_2\to B_2}$ can be rewritten as

$$P_{out}^{A_2\to B_2} = 1 - Pr\left(\frac{a_2\rho|h_{A_2}|^2}{a_1\rho|h_{A_1}|^2+1} > \gamma_{th}^{(2)}\right) \times Pr\left(\frac{b_1\rho|h_{B_2}|^2}{b_2\rho|h_{B_2}|^2+1} > \gamma_{th}^{(1)}, b_2\rho|h_{B_2}|^2 > \gamma_{th}^{(2)}\right) \quad \textbf{(B.1)}$$

$$= 1 - \underbrace{Pr\left(\frac{a_2|h_{A_2}|^2-\gamma_{th}^{(2)}/\rho}{a_1\gamma_{th}^{(2)}} > |h_{A_1}|^2\right)}_{\Theta_4}\underbrace{Pr\left(|h_{B_2}|^2 > \frac{\delta^*}{\rho}\right)}_{\Theta_5}$$

where $a_2 > a_1\gamma_{th}^{(1)}$ is always satisfied to maintain the implementation of NOMA protocol.

Thus, Θ_4 is given by (**A.4**) and Θ_5 is forwardly derived as

$$\Theta_5 = exp(-\tau^*/\rho)\sum_{k=0}^{m_{B_2}-1}\frac{1}{k!}(\tau^*/\rho)^k \quad \textbf{(B.2)}$$

Substituting Θ_4 and (**B.2**) into (**B.1**), (11) can be obtained.